HHS Public Access

Author manuscript

Arch Biochem Biophys. Author manuscript; available in PMC 2019 March 15.

Published in final edited form as:

Arch Biochem Biophys. 2019 March 15; 663: 22–33. doi:10.1016/j.abb.2018.12.017.

Muscle activity prevents the uncoupling of mitochondria from Ca^{2+} Release Units induced by ageing and disuse

Laura Pietrangelo[a], **Antonio Michelucci**[a,b], **Patrizia Ambrogini**[c], **Stefano Sartini**[c], **Flavia A. Guarnier**[a], **Aurora Fusella**[a], **Ilaria Zamparo**[d], **Cristina Mammucari**[d], **Feliciano Protasi**[e,1], and **Simona Boncompagni**[a,*,1]

[a]CeSI-Met - Center for Research on Ageing and Translational Medicine and DNICS - Dept. of Neuroscience, Imaging and Clinical Sciences, University G. d' Annunzio, I-66100, Italy

[b]Department of Pharmacology and Physiology, University of Rochester Medical Center, Rochester, NY, 14642, USA

[c]Dept. of Biomolecular Sciences, University of Urbino Carlo Bo, I-61029, Italy

[d]Dept. of Biomedical Sciences, University of Padova, I-35131, Italy

[e]CeSI-Met - Center for Research on Ageing and Translational Medicine and DMSI - Dept. of Medicine and Aging Sciences, University G. d'Annunzio of Chieti, I-66100, Italy

Abstract

In fast-twitch fibers from adult mice Ca^{2+} release units (CRUs, i.e. intracellular junctions of excitation-contraction coupling), and mitochondria are structurally linked to each other by small strands, named *tethers*. We recently showed that aging causes separation of a fraction of mitochondria from CRUs and a consequent impairment of the Ca^{2+} signaling between the two organelles. However, whether the uncoupling of mitochondria from CRUs is the result of aging *per-se* or the consequence of reduced muscle activity remains still unclear. Here we studied the association between mitochondria and CRUs: in a) *extensor digitorum longus* (EDL) muscles from 2 years old mice, either sedentary or trained for 1 year in wheel cages; and b) denervated EDL muscles from adult mice and rats. We analyzed muscle samples using a combination of structural (confocal and electron microscopy), biochemical (assessment of oxidative stress via western blot), and functional (*ex-vivo* contractile properties, and mitochondrial Ca^{2+} uptake) experimental

*Corresponding author. laura.pietrangelo@unich.it (L. Pietrangelo), antonio.michelucci@unich.it (A. Michelucci), patrizia.ambrogini@uniurb.it (P. Ambrogini), stefano.sartini@uniurb.it (S. Sartini), faguarnier@uel.br (F.A. Guarnier), aurora.fusella@gmail.com (A. Fusella), ilaria.zamparo@unipd.it (I. Zamparo), cristina.mammucari@unipd.it (C. Mammucari), feliciano.protasi@unich.it (F. Protasi), simona.boncompagni@unich.it (S. Boncompagni).

Author contributions

Feliciano Protasi and Simona Boncompagni conceived and directed the study. Laura Pietrangelo, Antonio Michelucci, Patrizia Ambrogini, Stefano Sartini, Flavia A. Guarnier, Aurora Fusella, Ilaria Zamparo, Cristina Mammucari, and Simona Boncompagni performed the experimental work and data analysis. In detail: a) LP performed all qualitative and quantitative EM studies; b) AF performed sectioning for EM and histology; c) SB performed confocal imaging; d) AM performed functional studies; e) PA and SS performed denervation experiments in rats; f) FAG performed measurements of oxidative stress; g) IZ e CM performed denervation experiments in mice and Ca^{2+} measurements. Finally, LP, AM, FP, and SB wrote the manuscript.

[1]Contributed equally to this work.

Conflict of interest

None.

Appendix A. Supplementary data

Supplementary data to this article can be found online at https://doi.org/10.1016/j.abb.2018.12.017.

procedures. The results collected in structural studies indicate that: a) ageing and denervation result in partial uncoupling between mitochondria and CRUs; b) exercise either maintains (in old mice) or restores (in transiently denervated rats) the association between the two organelles. Functional studies supported the hypothesis that CRU-mitochondria coupling is important for mitochondrial Ca^{2+} uptake, optimal force generation, and muscle performance. Taken together our results indicate that muscle activity maintains/improves proper association between CRUs and mitochondria.

Keywords

Excitation-contraction (EC) coupling; Sarcoplasmic reticulum (SR); Denervation; Exercise; Skeletal muscle; Electron microscopy

1. Introduction

Aging is a term describing a variety of physiological and morphological alterations occurring over life, characterized by a progressive and irreversible decline of biological functions affecting different organs and tissues [1]. Age-related decline in skeletal muscle performance has a major impact on mobility, independency, and quality of life of elderly people [2] and is characterized by a great reduction in muscle mass (i.e. sarcopenia), force development, and increased fatigability [3,4]. As the percentage of elderly people is increasing, and considering the related rise in health care costs [5], maintaining the efficiency of skeletal muscle with age would be crucial for improving the quality of life and independence of elderly individuals.

Skeletal muscle contraction is supported by two major intracellular organelles: Ca^{2+} release units (CRUs), or triads [6], and mitochondria. CRUs are the sites that mediate excitation-contraction (EC) coupling, the process whereby an action potential that travels along the transverse-tubule (TT) membrane triggers the release of Ca^{2+} from the sarcoplasmic reticulum (SR) [7]. At the molecular level, EC coupling is mediated by mechanical interaction between dihydropyridine receptors (DHPRs), the voltage sensors of TT membranes, and the ryanodine receptor type 1 (RyR1), the Ca^{2+} release channel located in the SR terminal cisternae [8]. Mitochondria are the "*powerhouses*" of the cell, being responsible for aerobic ATP production required mainly for myosin/actin cross-bridge cycle and for reuptake of Ca^{2+} by sarco/endoplasmic reticulum ATPases (SERCA) [9], during a contraction/relaxation cycle. We previously reported that in adult fast-twitch fibers, mitochondria and CRUs are physically linked to one another by small strands, referred to as *tethers* [10]. The tethering of mitochondria to CRUs has been proposed to restrict mitochondrial movement in the myoplasm, positioning them in close proximity (~160 nm) to sites of Ca^{2+} release (i.e. RyR1 release channels). This CRUs-mitochondria association maybe important for the Ca^{2+} signaling between the two organelles during EC coupling as the Ca^{2+} released from SR enters into the mitochondrial matrix to stimulate the respiratory chain and, hence, ATP production [11–13].

We have recently shown that proper association of mitochondria with CRUs is challenged in physio-pathological conditions such as denervation [14] and aging [15,16]. In Pietrangelo et

al., 2015 [15], we proposed that the age-related separation between the two organelles may contribute to the decline of skeletal muscle performance during ageing and we concluded that possible interventions designed to prevent uncoupling of mitochondria from CRUs could improve muscle function in the elderly.

The importance of physical activity in aged people has been largely studied and there is general agreement about its benefits [17]. Physical exercise is known to have beneficial effects on trophism, force and endurance of muscle, thus improving quality of life of elderly people [18,19]. Recently, we have also shown that lifelong physical activity could be indeed an effective strategy to counteract functional and structural decay of skeletal muscle in biopsies from athletically-active aged individuals [16]. In addition, we collected initial evidence that exercise may protect the proper triad-mitochondria association [16], an observation needing more rigorous and controlled studies in animal models. Specifically, two main issues remain to be fully elucidated: i) Age-related CRU-mitochondria uncoupling is the result of ageing *per-se* or reduced muscle activity contributes to these changes? ii) Is this process reversible?

Here, we analyzed the structure and function of muscles from WT mice trained in wheel cages for a period of 1 year (from 12 to 24 months of age) and compared them with those of adult and aged-matched untrained mice. We also performed studies in muscles obtained from mice and rats subjected to a period of denervation (which mimics muscle disuse). Our results revealed that muscle fibers from both aged mice and mice denervated for a period of 3 or 14 days, display a significant reduction in mitochondria volume and number, an increased frequency of misplaced mitochondria and a significant decrease in CRUs/mitochondria pairs. These changes were accompanied by: a) impairment in muscle strength; b) increased oxidative stress; c) reduced mitochondrial Ca^{2+} uptake.

Worthy of special note is the fact that 1 year of voluntary running in wheel cages in mice and reinnervation in rats: a) counteracted the loss of mitochondria; b) reduced the number of misplaced mitochondria and c) restored the coupling between mitochondria and CRUs.

2. Material and methods

2.1. Animals

All procedures and experiments in this study were conducted according to National Committee for the protection of animals used for scientific purposes (D. lgs n.26/2014). Animals were housed in microisolator cages at 20 °C in a 12-h light/dark cycle and provided free access to standard chow and water. All surgeries were made to minimize animal suffering and animals were sacrificed by cervical dislocation as approved by the D. lgs n. 26/2014. Wild type (WT) male C57bl/6 mice and WT male CD1 mice were housed in the animal facility of University of Chieti and Padova, respectively. WT male Sprague Dawley rats were housed in the animal facility of University of Urbino and sacrificed by an overdose of sodium thiopental via intraperitoneal (i.p.) injection.

2.2. In-vivo experiments

a) Exercise protocol. C57bl6 WT mice of 12 months of age were randomly assigned to two experimental groups: aged mice (housed for 12 months in regular cages) and aged-trained mice (housed for 12 months in wheel cages for voluntary running). Aged-trained mice were individually accommodated in a 16 Station Home Cage Running Wheel System with CMI Software (Columbus Instruments, Columbus, OH, USA) and had free access to standard chow and water. Running activity of mice was monitored for all cages through a magnetic indicator and a sensor connected to a PC by a hub. Number of rotations performed each hour in each cage was recorded. Animals were then sacrificed at 24 months of age. *b) Denervation of mice and rats*: 1) At 6 months of age WT male CD1 mice were anesthetized and denervated by sciatic nerve section from one hindlimb. Wounds were closed with surgical staples and the mice were monitored for infection. Animals were then sacrificed after either 3 or 14 days from denervation. 2) WT male Sprague Dawley rats at 45 ± 5 days of age were anesthetized by an i.p. injection of sodium thiopental (45 mg/kg b.w.), the left sciatic nerve was exposed and crushed distally to the inferior gluteal branch to induce hindlimb muscle denervation, and then allowed to recover. Animals were sacrificed either at 15 (denervated) or 45 days (reinnervated) after nerve crush.

2.3. Preparation and analysis of samples for histology and electron microscopy (EM)

EDL muscles were quickly dissected from sacrificed mice or rats, pinned on Sylgard dishes, fixed at room temperature with 3.5% glutaraldehyde in 0.1 M NaCaCO buffer (pH 7.2), and stored in the fixative at 4 °C before embedding. Fixed muscles were then post-fixed, embedded, stained en-block, as described previously [15]. For TT staining, specimens were post-fixed in a mixture of 2% OsO_4 and 0.8% $K_3Fe(CN)_6$ for 1–2 h followed by a rinse with 0.1M NaCaCO buffer with 75 mM $CaCl_2$. For histological examination, 700 nm thick sections were stained in a solution containing 1% Toludine blue O and 1% Sodium Borate Tetra in distilled water for 3 min on a hot plate at 55–60 °C. After washing and drying, sections were mounted with DPX mounting medium for Histology (Sigma-Aldrich, Milan, Italy) and observed with a Leica DMLB light microscope (Leica Microsystem, Vienna, Austria). For EM, ultrathin sections (~50 nm) were cut using a Leica Ultracut R microtome (Leica Microsystem, Vienna, Austria) with a Diatome diamond knife (Diatome, Biel, Switzerland) and double-stained with uranyl acetate and lead citrate. Sections were viewed in a FP 505 Morgagni Series 268D electron microscope (FEI Company, Brno, Czech Republic), equipped with Megaview III digital camera (Olympus Soft Imaging Solutions, Munster, Germany) and Soft Imaging System at 60 kV.

2.4. Immunofluorescence (IF) labeling and confocal microscopy

EDL muscles were dissected from sacrificed animals, fixed in 2% paraformaldehyde in phosphate buffered saline (PBS) for 20 min at room temperature and stored at 4 °C overnight. Small bundles of fixed EDL fibers were washed three times in PBS containing 1% bovine serum albumin (PBS/BSA) and incubated in blocking solution (PBS/BSA with 10% goat serum and 0.5% Triton X-100) for 1 h at RT, followed by an overnight incubation at 4 °C with one of the following primary antibodies: a) mouse monoclonal anti-RYR1 (34C, dilution 1:30; Developmental Studies Hybridoma Bank University of Iowa, Iowa City,

Iowa), b) rabbit polyclonal anti-translocase of outer mitochondrial membrane 20 homolog (TOM20, dilution 1:100; Santa Cruz Dallas, TX). Muscle bundles where then washed three times in PBS/BSA and then incubated for 1 hr at RT with the appropriate secondary antibodies: a) Cy5-labeled goat anti-mouse IgG (dilution 1:50); or b) Cy3-labeled goat anti-rabbit (dilution 1:200). All secondary antibodies were purchased from Jackson ImmunoResearch Laboratories (Lexington, KY). Confocal images were acquired using a Zeiss LSM510 META laser-scanning confocal microscope system (Zeiss, Jena, Germany) equipped with a Zeiss Axiovert 200 inverted microscope and a Plan Neofluar oil-immersion objective (100X/1.3 NA).

2.5. Quantitative analyses by EM

For all quantitative EM analyses micrographs of non-overlapping regions were randomly collected from transversal and longitudinal sections of internal areas of EDL fibers. See Figures and Supplemental tables for additional details about sample size.

1. Number of CRUs/area was evaluated in longitudinal sections and reported as average number/100 μm^2. In each EM image, we also determined the orientation of CRUs (oblique and longitudinal) and the percentage of dyads.

2. Number of mitochondria and mitochondria-CRUs pairs/area were evaluated in longitudinal sections and reported as average number/100 μm^2 (see Boncompagni et al., 2009 [10] for additional detail). In each EM image, we also determined the mitochondrial positioning with respect to the I and A bands. If an individual mitochondrion extended from one I band to another, it was counted in both.

3. Mitochondrial volume was determined using the well-established stereology point-counting technique [20,21] in micrographs taken from transversal sections at magnification 7.100–8.900X. Briefly, after superimposing an orthogonal array of dots at a spacing of 0.20 μm to the electron micrographs, the ratio between numbers of dots falling within mitochondrial profiles and total number of dots covering the whole image was used to calculate the relative fiber volume occupied by mitochondria.

4. Z-line misalignments was evaluated in micrographs taken from longitudinal sections of internal fiber areas, from aged and aged-trained mice at 7.100–14.000X of magnification. In each EM image we determined the number of disordered myofibrils presenting one or more sarcomeric units with misalignments of Z line with respect to the upper and lower myofibrils. We evaluated the number as percentage of the total counted myofibrils.

2.6. Quantitative histological analysis

EDL muscles from aged and aged-trained mice and those form control, denervated (15 days from nerve crush) and re-innervated (45 days from nerve crash) rats were sectioned both transversally and longitudinally. Images were acquired using a Leica DMLB microscope (Leica Microsystem, Vienna, Austria) connected to a Leica DFC450 camera (Leica Microsystem, Vienna, Austria).

1. We measured cross sectional area (CSA) of EDL fibers of aged and aged-trained mice and those from control, denervated and reinnervated rats in transversal semithin sections using Leica Application Suite v 4.6 for Windows (Leica Microsystem, Vienna, Austria).
2. We classified muscle fibers from control, denervated and reinnervated rats as *normal or altered* based on the absence or presence of areas in which cross striation was lost.

2.7. Grip strength test

As a standard procedure, weight and grip strength were recorded for aged and aged-trained mice. Force developed by mice during instinctive grasp (i.e. grip strength) was measured as described in Connolly et al., 2001 [22]. Briefly, mice were held by the tail and lowered to a metal grating connected to the shaft of a Shimpo Fgv 0.5x force transducer (Metrotec Group, Lezo, Spain). Once the mouse had firmly grabbed the grating, a steady, gentle pull was exerted on the tail. Measurements of peak force generated by each mouse using fore- and hind-limbs were repeated three times with appropriate intervals (at least 30 s) to avoid fatigue and the highest value of peak force measured was used.

2.8. Ex-vivo contractile protocol

EDL muscles were rapidly removed from hind limbs of aged and aged-trained mice, and immersed in a Krebs-Henseleit (KH) solution containing: 118 mM NaCl; 4.7 mM KCl; 1.2 mM $MgSO_4$; 2.5 mM $CaCl_2$; 1.2 mM KH_2PO_4; 25 mM $NaHCO_3$; 11 mM glucose. Muscles were pinned and tied with fine silk sutures at each end. Muscles were mounted vertically between two platinum electrodes immersed in an organ chamber filled with KH solution and attached to a servo motor and force transducer (model 1200A, Aurora Scientific, Aurora, ON, Canada) as in Boncompagni & Michelucci et al., 2017 [23]. Before starting the experimental protocol, stimulation level and optimal muscle length (L_0) were determined using a series of 80 Hz-tetani in order to stretch the muscle to the length that generated maximal force (P_0). Once both L_0 and P_0 were reached, EDL muscles were subjected to a force-frequency protocol based on a series of train pulses of 500 ms duration each as follows (in Hz): 1, 5, 10, 20, 40, 60, 80, 100, 120, and 140. After waiting 5 min to allow muscles to recover from the force-frequency protocol, the same EDL muscles were subjected to a single-sustained high frequency tetanus (120 Hz, 2 sec) to record the maximal force developed by muscles. The frequency used for the 2 sec tetanus, was chosen as the lower frequency able to produce the maximal force, as observed by the analysis of the force-frequency curve. All experiments were performed at 25 °C. Muscle force was recorded using a dynamic muscle control (DMC) and analyzed using dynamic muscle analysis (DMA) software (Aurora Scientific, Aurora, ON, Canada). Specific force (mN/mm^2) was calculated by normalizing the absolute force (mN) to the physiological cross sectional area (mm^2) obtained as following: wet weight (mg)/L_0 (mm)* 1.06 (mg/mm^3)*0.44.

2.9. Western blot (WB) analyses

WB experiments were performed as previously described [24,25] to assess the amount of 3-nitrotyrosine (3-NT) and expression levels of Cu/Zn superoxide dismutase (SOD1) and Mn

superoxide dismutase (SOD2). Briefly, total hindlimb muscles obtained from aged (n = 3) and aged-trained (n = 3) mice were homogenized in lysis buffer containing 0.1 M TRIS-HCl (pH 7.2), 0.2% SDS, 0.1% sodium deoxycolate, and 0.3M NaCl, and centrifuged for 15 min at 900×g at RT. Total protein quantification was performed by using Bradford method. 20 μg of total protein were separated in 12% sodium dodecyl sulphate-polyacrylamide gel electrophoresis (SDS-PAGE) and transferred to nitrocellulose membrane. Membranes were probed using primary antibodies against SOD1 (rabbit polyclonal, dilution 1:1000; Santa Cruz Biotecnology, Dallas, TX), SOD2 (rabbit polyclonal, dilution 1:2000; Santa Cruz Biotecnology, Dallas, TX), 3-NT (mouse monoclonal, dilution 1:500; Merck Millipore, Darmstadt, Germany), and glyceraldehyde-3-phosphate dehydrogenase (GAPDH) (mouse monoclonal, dilution 1:10000; OriGene Technologies, Rockville, MD), diluted in 10% non-fat dry milk in TBS-T overnight at 4 °C. Horseradish peroxidise (HRP)-conjugated anti-mouse or -rabbit (dilution 1:10000, Merck Millipore, Darmstadt, Germany) were used as secondary antibodies. Peroxidase activity was detected using an Enhanced chemiluminescence (ECL) kit (Perkin Elmer, Waltham, MA). The bands were visualized using a gel documentation system (UVItec, Cambridge, UK), and the band densitometric quantification of signals was performed using Image J software (National Institute of Health, Bethesda, MA). Specifically, for the assessment of 3-NT levels, we quantified and averaged by densitometric analysis the combined intensities of both 55 and 25 KDa bands. The values obtained were then averaged and normalized to those of GAPDH used as a loading control.

2.10. Ca^{2+} imaging in single flexor digitorum brevis (FDB) fibers

FDB muscles were dissected from denervated (n = 3 for each time points) and control mice (n = 2). Muscles were then digested in type I collagenase (6 mg/ml), and single fibers plated on laminin-coated coverslips and cultured in Dulbecco's modified eagle medium (DMEM) containing 10% fetal bovine serum (FBS), 50 U/ml penicillin, 50 mg/ml streptomycin (Sigma-Aldrich, Milan, Italy). Imaging of fibers was performed using an Olympus IX 71 inverted microscope (Olympus Corporation, Tokio, Japan) equipped with a PlanApo 60x/1.4 N.A. oil immersion objective, a xenon light source (75W) for epifluorescence illumination and a 12-bit digital cooled CCD camera (Micromax, Princeton Instruments, New Jersey Trenton, NJ). Data were acquired using Cell R Software (Olympus Corporation, Tokio, Japan). During the experiments, FDB fibers were maintained in Krebs-Ringer modified buffer (135 mM NaCl, 5 mM KCl, 1 mM $MgCl_2$, 20 mM HEPES, 1 mM $MgSO_4$, 0.4 mM KH_2PO_4, 1 mM $CaCl_2$, 5.5 mM glucose, pH 7.4) at RT, in presence of 75 μM N-benzyl-P-toluenesulfonamide (BTS, Sigma-Aldrich, Milan, Italy) to avoid fiber contraction. For mitochondrial Ca^{2+} measurements, FDB muscles were transfected with a genetically-encoded Ca^{2+}-sensitive probe targeted to mitochondria (4 mt-GCaMP6m) as previously reported [26]. 4 mt-GCaMP6m was alternatively excited through 490/20 and 403/20 nm band-pass excitation filters and images were collected through a 460/15–525/25–630/15 nm triple-band emission filter (Olympus corporation, Tokio, Japan). Exposure time and lamp were set to 50 ms to 6.85% of the maximum power, respectively, and images were acquired every 3 s. Changes in Ca^{2+} levels (490/403 nm fluorescence ratio) were expressed as R/R0, where R is the ratio at time t and R0 is the ratio at the beginning of the experiment. Analysis was performed with the Fiji distribution [27] of Image J software (National Institute of

Health, Bethesda, MA). Images were background corrected frame by frame by subtracting the mean pixel value of a cell-free region of interest.

For cytosolic Ca^{2+} measurements FDB fibers were loaded with 2 μM Fura-2/AM (Life Technologies, Carlsbad, California) diluted in Krebs-Ringer modified buffer containing 0.02% pluronic acid for 20 min at 37 °C and then washed with Krebs-Ringer modified buffer. 10 mM caffeine (Sigma-Aldrich, Milan, Italy) was added when indicated to elicit Ca^{2+} release from intracellular stores. Images were acquired every 3 sec with a UApo/340 40x/1.35 N.A. oil immersion objective (Olympus corporation, Tokio, Japan) using 380/15 nm and 340/15 nm band-pass excitation filters and collected through a 460/15–525/25–630/15 nm triple-band filter (Olympus corporation, Tokio, Japan). Exposure time was set to 200 ms and the lamp was set to the 26.17% of the maximum power. Changes in fluorescence (340/380 nm ratio) was expressed as R/R0, where R is the ratio at time t and R0 is the ratio at the beginning of the experiment.

2.11. Statistical analyses

Statistical significance in all experiments was evaluated using a two-tailed unpaired Student's *t*-test, except for the ex-vivo force-frequency experiments, the histological analysis of the percentage of altered EDL muscle fibers from rats, and the EM analysis of EDL muscles from rats, in which significance was evaluated using repeated measurements ANOVA followed by post-hoc Tuckey test, one-way ANOVA followed by *post-hoc* Tuckey test, and Fischer's exact text, respectively. All data were presented as mean ± SEM. Statistical significance was considered for values of $p < 0.05$.

3. Results

3.1. Exercise prevents age-related changes in the disposition of mitochondria, and improves function and oxidative capacity of muscle

We compared two groups of 2 year aged mice: sedentary (aged) vs. aged subjected to 1 year of voluntary running in wheel cages (aged-trained).

3.1.1. Exercise maintains the structural association between mitochondria and CRUs in aged mice—We first analyzed EDL muscles using a combination of IF and EM. In IF experiments, CRUs were marked with an antibody that recognizes RyR1, while the position of mitochondria was detected using an antibody that labels TOM20. This co-immunostaining resulted in typical cross striation of CRUs with adjacent mitochondria, located within the I band region of the sarcomere [10,15]. The precise cross striation was partially lost in some areas of the fiber (Fig. 1 A, inset; see also Fig. S1 A–C), with some mitochondria staining that exhibits longitudinal orientation (see Pietrangelo et al., 2015 for additional detail [15]). These areas reflect those regions visible in EM in which: i) mitochondria distribution formed clusters and/or longitudinal columns between the myofibrils (Fig. 1C, empty arrow); and ii) TTs [15], exhibited partial disarray and also a longitudinal orientation (Fig. 1 E, arrowheads). This loss of TT system organization might be the result of lateral misalignment of myofibrils, a condition detected in ~40% of EDL fibers at 2 years of age (Fig. 1 E).

Analysis of EDL muscles from aged-trained mice revealed that voluntary exercise significantly improved the overall appearance of fibers, with the regular cross striation pattern of fluorescence that was restored in the majority of analyzed tissue (Fig. 1 B; see also Fig. S1 D–F). In line with the observations made in IF experiments, EM analysis supported this finding, as only 18% of fibers from aged-trained mice showed sign of lateral misalignment of myofibrils, a value significantly reduced compared to that of aged mice (~40%). Disposition of mitochondria and TTs (Fig. 1 D and F) was virtually indistinguishable from that of adult fibers, with most mitochondria correctly positioned within the I band of the sarcomere on each side of the Z-line (Fig. 1 D, arrows) and TT, stained in black in Fig. 1 F (arrowheads), transversally oriented with respect to the main axis of myofibrils. See Boncompagni et al., 2009 and Pietrangelo et al., 2015 for details about the specific disposition of CRUs and mitochondria in adult EDL skeletal muscle [10,15].

The quantitative analysis shown in Fig. 1 G–L and Table S1 confirmed the visual observations. While ageing causes a partial misplacement of mitochondria from the I band region, 1 year of voluntary running was able to: i) increase the number of mitochondria per area and the mitochondrial volume (Fig. 1 G and H); ii) decrease the number of mitochondria improperly placed at the A band (Fig. 1 I); iii) improve association of mitochondria to CRUs (Fig. 1 L). See Table S1 for numeric values of data in Fig. 1 G–L. The increased CRU/mitochondria association (Fig. 1 L) is the combined consequence of i) the improved number and disposition of mitochondria (Fig. 1 G–I) and b) the positive effect that training exerted also on structure and positioning of triads (Table 1): indeed, in aged-trained mice, n./area of CRUs was increased (Table 1, column A), while the frequency of oblique, longitudinal, and incomplete (i.e. dyads) CRUs were all decreased (Table 1, columns B-D).

3.1.2. Exercise improves in-vivo grip strength and ex-vivo muscle contractile function in aged mice—To evaluate whether voluntary exercise was able to improve the functional output, we measured *in-vivo* grip strength and *ex-vivo* contractile force in aged and aged-trained mice after determining body weight and CSA of EDL fibers. Body weight of trained mice (29.9 ± 0.5 gr) was significantly reduced compared to that of aged-matched untrained mice (33.9 ± 1.5 gr; Fig. 2A), while CSA of EDL fibers was slightly, but significantly, increased (1244 ± 21 μm^2 vs. 1116 ± 18 μm^2) (Fig. S2 C). The distribution frequency of EDL fibers CSA (Fig. S2 D) shows a right shift of CSA in trained animal, i.e. toward fibers of greater diameter. The decreased body weight combined with the increased CSA of EDL fibers suggest a possible reduction of body fat in trained animals (Fig. S2).

In-vivo grip strength test indicated that both absolute and specific force were increased of about 14% and 25%, respectively in trained mice vs. untrained controls, a difference that was statistically significant (Fig. 2 B and C).

We then assessed *ex-vivo* contractile force in isolated intact EDL muscles by measuring force-frequency and 2 sec tetanic force (Fig. 2D–F). The force-frequency relationship curve showed that EDL muscles from aged-trained mice developed a specific force significantly higher than that from control mice during high-frequency stimulation from 80 to 140 Hz (Fig. 2 D). No difference was detected in the relative force-frequency curve, normalized to

the maximal force (F_0) (Fig. 2 E). The absence of a leftward or rightward shift of the relative force-frequency curve in muscles from trained aged mice compared to muscles of aged mice, suggests that 1 year of voluntary running did not change the fiber type composition in EDL muscles from aged-trained mice. Indeed slow-twitch fibers would generate a higher force at lowers frequencies than fast-twitch fibers, as the consequence of the different myosin heavy chain isoform expression (type I in slow twitch vs. type IIx/IId in fast-twitch fibers) and the slower kinetic of SR Ca^{2+} release and re-uptake cycle [28].

We finally evaluated also the maximal force developed by the same EDL muscles by applying a single 2 sec-stimulus train elicited at 120 Hz to generate a fused tetanus (Fig. 2 F). EDL muscles from aged trained mice exhibited a maximal specific force significantly higher to that developed by EDL muscles from aged mice (208.4 ± 10.7 vs. 176.2 ± 6.9 mN/mm).

3.1.3. Exercise reduces oxidative stress in skeletal muscle of aged-trained mice—

We previously showed that oxidative stress was elevated in aged muscle [15]. Here, we assessed levels of: i) 3-Nitrotyrosine (3-NT), a byproduct of nitration of protein tyrosine residues mediated by RNS such as peroxynitrite and nitrogen dioxide [29–32]; and ii) superoxide dismutase 1 and 2 (SOD1 and SOD2), the two main intracellular enzymes, respectively, localized in the cytoplasm and within mitochondrial matrix, that catalyze the dismutation of superoxide anion ($O^{\bullet -}_2$) into O_2 and hydrogen peroxide (H_2O_2) [33–35]. Analyses by WB revealed that the amount of 3-NT (Fig. 3 A and B) was significantly lower in aged-trained compared to controls (1.32 ± 0.07 *vs* 1.56 ± 0.12 arbitrary units). In the same samples, SOD2 were ~15% higher in aged-trained than in controls (Fig. 3 E and F), while no differences were observed in SOD1 levels (Fig. 3 C and D).

3.2. Denervation results in uncoupling of mitochondria from CRUs in adult mice

To further investigate whether the intracellular disarray of the mitochondrial apparatus in muscle fibers was due to ageing itself or to disuse of muscle (i.e. inactivity), we studied muscles from adult mice (6 months) at 3 and 14 days of denervation.

3.2.1. Muscle inactivity leads to mitochondria misplacement from the I band and loss of mitochondria/CRUs pairs in adult mice—

Muscle paralysis following denervation induced modifications in the intracellular positioning of mitochondria similar to those encountered in aged mice. We evaluated by EM the mitochondrial n./area, volume, disposition, and association with CRUs (Fig. 4). Changes in mitochondrial disposition were visible after only 3 days of denervation to become more evident after 14 days (Fig. 4 A–C). While mitochondria are preferentially located at I band in control fibers (Fig. 4 A, arrows), an increased number of mitochondria becomes longitudinally oriented following denervation (Fig. 4 B and C, empty arrows). Quantitative analysis in Fig. 4 D–G and Table S2 showed that in denervated muscles: a) n./area of mitochondria significantly decreased after 3 and 14 days of denervation compared to control muscles (Fig. 4 D and Table S2, column A), although mitochondrial volume (relative to the total fiber volume) was unchanged (Fig. 4 E and Table S2, column B), possibly due to a concomitant atrophy of the contractile apparatus (Fig. 4 E and Table S2, column B); b) the number of mitochondria at the A band of the

sarcomere (i.e. improperly positioned) was greatly increased with denervation (Fig. 4 F and Table S2, column C); and finally c) the proper association between mitochondria and CRUs was significantly reduced of about 20% at 3 days and 50% at 14 days (Fig. 4 G and Table S2, column D). Similar to that observed in aged muscle (Table 1) the reduced CRUs/mitochondria association following denervation may represent the combined effect of changes in mitochondria and of structure/positioning of CRUs (Table 2): n./area was decreased after 3 and 14 days of denervation (Table 2, column A), while the frequency of oblique, longitudinal, and incomplete (i.e. dyads) CRUs were all increased (Table 2, columns B-D).

3.2.2. Muscle inactivity impairs mitochondrial Ca^{2+} uptake in FDB fibers of denervated mice—

We previously reported that the disruption of CRUs/mitochondria association in aged fibers, reduces the ability of mitochondria to uptake Ca^{2+} ions, released during EC-coupling [15]. Since the association between mitochondria and CRUs was partially disrupted by denervation (Fig. 4), here we evaluated mitochondrial Ca^{2+} uptake in single isolated FDB fibers from mice subjected to 3 and 14 days of denervation. After 3 days of denervation FDB fibers exhibited a reduced mitochondrial Ca^{2+} uptake (Fig. 5 A and C), but basically unaltered cytosolic Ca^{2+} transients (Fig. 5 B and D) compared to control fibers. Surprisingly, although the further decrease of CRUs/mitochondria pairs observed in EM after 14 days after denervation, both mitochondrial (Fig. 5 A and C) and cytosolic Ca^{2+} transients were significantly enhanced (Fig. 5 B and D). The latter finding was unexpected and will be addressed in Discussion.

3.3. Reinnervation reverses mitochondria/CRUs uncoupling in adult rats

To test if the uncoupling between CRUs and mitochondria caused by denervation is a reversible process, we used a transient model of denervation: sciatic nerve crush in adult rat. EDL muscles were studied in histology, IF, and EM either after 15 (a stage in which muscle are still denervated) or 45 days (a time sufficient to allow re-innervation of muscle fibers) from the crash of sciatic nerve.

3.3.1. Reinnervation restores the morphometric and morphological appearance of muscle fibers in rats—

Using histological images EDL muscles from control, denervated, and reinnervated rats, we measured: i) the cross sectional areas (CSA) in transversal sections (Fig. 6 A–C and G); ii) and the percentage of fibers presenting areas loosing cross striation and/or a clear disarray of the contractile elements, in longitudinal histological sections (Fig. 6 D–F and H). The analysis of the frequency distribution for CSA, revealed that the majority of fibers in muscles from control rats have an average CSA value of $2.2 \pm 0.1\ \mu m^2 \times 10^3$ (Fig. 6 G, black columns); after 15 days of denervation, the average CSA of fibers was greatly reduced to a value of $0.8 \pm 0\ \mu m^2 \times 10^3$, as also shown by the leftward shift of the frequency distribution curve (Fig. 6 G, red columns). The increased number of fibers with a smaller size is a typical sign of denervation-induced atrophy. After reinnervation, the average fiber CSA value was $1.4 \pm 0.1\ \mu m^2 \times 10^3$ accompanied by a rightward shift of the fiber size distribution toward the control (Fig. 6 G, blue columns).

Using longitudinal sections, we also analyzed and classified fibers in two different categories (Fig. 6 D–F): a) *normal* fibers, presenting a well preserved cross-striation pattern; and b) *altered* fibers, showing internal areas with disarray of their striated appearance (marked with asterisks in Fig. 6 E). Quantitative analysis of the relative percentage of fibers falling in the two different categories (Fig. 6 H) indicated that re-innervation was effective in restoring muscle structure, as *altered* fibers, abundant in EDL muscles from denervated rats (about 40%), decreased following reinnervation (6.9%) to a percentage very close to that of control muscles (4.4%) (Fig. 6 H).

3.3.2. Re-innervation restores mitochondria n./area, intracellular disposition, and association with CRUs—We used IF and EM analyses to determine n./area, volume, and intracellular disposition of mitochondria in EDL muscles from control (Fig. 7 A and B), denervated (Fig. 7 C and D), reinnervated rats (Fig. 7 E and F). In adult skeletal muscle fibers from WT rats both CRUs (marked with an antibody that recognized RyR1, red fluorescence signal) and mitochondria (marked with an antibody that labeled TOM20, green fluorescence signal) formed the typical cross striations (Fig. 7 A and inset; see also Fig. S3 A–C), identical to that described in mice (see Fig. 1). This staining reflected the ordered disposition of CRUs and mitochondria visible in EM (Fig. 7 B, arrows). In denervated skeletal muscle fibers, this ordered disposition is compromised, with the green fluorescence signal of mitochondria often being longitudinal (Fig. 7 B and inset; see also Fig. S3 D–F). These areas reflect those regions visible in EM in which mitochondria, uncoupled from CRUs, display a longitudinal distribution forming columns between the myofibrils (Fig. 7 D, empty arrow). Worthy of note, reinnervation completely restored the normal appearance of skeletal fibers: confocal images show that the normal cross striations of CRUs (red signal) with adjacent mitochondria (green signal) within the I band (Fig. 1 E and inset; Fig. S3 G–I). In parallel EM examination showed that mitochondria are in close proximity to CRUs and form a row on each side of the Z-line (Fig. 7 F, arrows).

The qualitative observations were supported by quantitative EM analyses showing how most structural alterations induced by denervation were reverted by reinnervation: i) increased n./area of mitochondria (Fig. 7 G and Table S3, column A); ii) reduced number of misplaced mitochondria (Fig. 7 I and Table S3, column C); iii) increased the association between mitochondria and CRUs (Fig. 7 L and Table S3, column D). The only parameter that was not rescued by reinnervation was the mitochondrial volume (Fig. 7 H and Table S3, column B).

4. Discussion

4.1. Main findings of the study

In 2015 we provided evidence that: a) the structural association between CRUs and mitochondria is compromised in skeletal muscle fibers from aged mice [15]; b) CRU-mitochondria association is better preserved in biopsies of athletically-active than in age-matched individuals [16]. The latter finding suggests that aerobic exercise could be an effective strategy to counteract age-dependant uncoupling of mitochondria from CRUs.

Here we performed a study in which we evaluated the effect of ageing, exercise, denervation, and re-innervation on the association between mitochondria and CRUs to

determine if: a) ageing *per-se* is the leading cause of CRU-mitochondria uncoupling or, else, the reduced muscle activity associated with ageing is the main cause; and b) the misplacement of mitochondria for their correct position is a reversible phenomenon. The results of this study suggest that reduced activity is the main cause of separation of mitochondria from CRUs, as: i) in exercised aged mice (2 years of age) the CRU-mitochondria association is better preserved than in aged-matched sedentary mice; ii) denervation induces misplacement of mitochondria, mimicking the effects of ageing, also in adult muscle. Finally, our experiments suggest that CRU-mitochondria uncoupling is reversible, as reinnervation of denervated muscle rescued the proper positioning of mitochondria next to site of Ca^{2+} release.

4.2. Age-related uncoupling of mitochondria from CRUs and excessive oxidative stress are prevented by regular exercise

The analysis of biopsies from elderly subjects revealed that proper association between CRUs and mitochondria is better preserved in individuals that regularly exercised in their life [16]. Here we reinforced those findings showing how the proper positioning of mitochondria next to CRUs is better maintained in exercised aged mice: number/area of mitochondria, number of CRUs, and the frequency of mito-CRU pairs are indeed increased, while the percentage of mitochondria miss-placed at the A band is lowered (Fig. 1 and Table S1). This structural organization of organelles involved in Ca^{2+} handling and aerobic ATP production likely contributes to the improved skeletal muscle function shown in Fig. 2. We recently reported that nitration of protein tyrosine residues (3-NT), as well as SOD1 and SOD2 expression were both increased in skeletal muscle from aged mice compared to young controls and used these findings to propose that oxidative stress may play a role on CRU-mitochondria coupling disruption [15]. Data in Fig. 3 showed that exercise effectively reduced 3-NT levels and increased SOD2 expression (the mitochondrial SOD isoform), supporting the idea that reduced levels of oxidative stress may contribute to maintain the proper association between mitochondria and CRUs. Exercise also reduced oxidative stress levels, increasing the expression of SOD2. Increase in SOD2 expression could be explained by the increase in mitochondrial number and volume (Fig. 1) [36–38], while less straight forward is the interpretation of the unchanged levels of SOD1 (Fig. 3). The data in Fig. 3 support the existing literature indicating that regular/moderate exercise induces an antioxidant defense by enhancing the activity of endogenous antioxidant enzymes such as SODs, glutathione peroxidase and catalase [39,40].

4.3. Muscle inactivity causes CRU-mitochondria uncoupling in muscle of adult mice

The results collected in Fig. 1 leaves one question unanswered: CRU-mitochondria uncoupling only occurs with ageing, or reduced muscle activity would have the same effect also in adult muscle? To test this hypothesis we denervated adult mice and young rats (6 months of age mice; 1.5 months old rats) and found that muscle paralysis in the lower limbs (causing complete lack of muscle movements) significantly reduced the number of mitochondria-CRUs pairs, mimicking the effect of ageing (Figs. 4 and 7; Tables S2 and S3). The misplacement of mitochondria from the triadic position observed in this study is in line with data obtained in denervated rabbits [14]. The partial loss of connection between the two organelles can be explained in part by the increased number of mitochondria at the A band,

and in part also by the decreased number of mitochondria and CRUs (Fig. 4 and Table 2). In Fig. 5 we also show that the inactivity-induced uncoupling between CRU and mitochondria, also affected mitochondrial Ca^{2+} dynamics. Mitochondrial Ca^{2+} uptake plays a pivotal role in the control of muscle metabolism and energy production required for contraction [26]. It has been reported that mitochondria take up Ca^{2+} very quickly during muscle stimulation [41], likely the consequence of the close proximity between mitochondria and Ca^{2+} release sites resulting in formation of microdomains of high [Ca^{2+}] between their membranes [42]. Measurements of mitochondrial Ca^{2+} uptake in single FDB fibers transiently expressing a Ca^{2+} sensitive probe (GCaMP6m) targeted to mitochondria, confirmed how mitochondria efficiently take up Ca^{2+} upon SR release [26]. On the other hand, we have also shown that triadic and longitudinal mitochondria, whose localization in reference to CRUs is substantially different, display similar Ca^{2+}–uptake following repetitive tetanic stimulation, suggesting that mitochondrial Ca^{2+} uptake in skeletal fibers might be more sensitive to global cytosol Ca^{2+} transients, than to local [Ca^{2+}] in microdomains [13]. The data in Fig. 5 of the present manuscript are not conclusive in discriminating the effect of local microdomains vs. global cytosolic transients. Indeed, while the number of CRU-mitochondria pairs is decreased (and the percentage of mitochondria at the A band is increased) both at 3 and 14 days of denervation, mitochondrial Ca^{2+} uptake is decreased at 3 days of denervation, but augmented at 14 days (Fig. 5). The interpretation of caffeine-induced Ca^{2+} release and mitochondrial Ca^{2+} uptake data at 14 days of denervation is not straight forward. One possible interpretation is that Ca^{2+} accumulates in the myoplasm after caffeine-induced release due to impaired SR re-uptake, a phenomena that could in turn underline the excessive mitochondrial uptake. However, the interpretation of this result would require additional experiments aiming to assess the expression levels of proteins involved in both SR and mitochondrial Ca^{2+} uptake (SERCA and Mitochodrial Ca^{2+} Uniporter, MCU), a task that, falls outside the main scope of the present work.

4.4. CRU-mitochondria un-coupling is reversible

We also provide evidence that the altered association between mitochondria and CRUs caused by muscle denervation is restored once muscle becomes active again. Indeed data in Fig. 7 (and Table S3) show how denervation in rats results both in misplacement of mitochondria and decrease in n./area of CRU-mitochondria pair. However, when enough time is given to the nerve to re-connect with muscles (i.e. 45 days after nerve crush), all mitochondrial parameters were rescued to control values. While the loss of proper mitochondrial position with denervation was previously reported [14,43–45], the rescued targeting of mitochondria to I band following reinnervation was not previously shown. The molecular bases of mitochondria association to triads are still unknown. In 2009 we described little bridges termed *tethers* [10], that may play a role in holding mitochondria in proximity of CRUs. Mitochondrial morphology is maintained by a proper balance between fusion and fission events [46]. Mitofusin (Mfn) is a transmembrane GTPase that coordinates fusion of the mitochondrial outer membranes [47], that comes into two isoforms: Mfn1 which is located in the mitochondrial outer membrane, and Mfn2, found in both the outer mitochondrial membrane and the ER/SR membrane [47–49]. In non-excitable cells, tethers seem to form thanks to an interaction between Mfn1 and Mfn2 proteins connected via their

C termini [47] and we proposed mitofusin-2 (Mfn2) is indeed a possible *tether* candidate also in skeletal muscle fibers [50].

5. Conclusion

Although science has never come close to stop humans from ageing, a big effort is put into advancing the understanding on how aging is regulated at the molecular and cellular levels in order to provide useful information to improve quality of life and independence of elderlies.

This study (Fig. 8): a) reveals that muscle activity maintains the correct association between CRUs and mitochondria, which is challenged by reduced muscle activity, even during ageing; b) identifies a novel (and potentially important) adaptation mechanism induced by exercise. As proper cross-talk between CRUs and mitochondria leads to efficient aerobic ATP production [9], restoration of CRU-mitochondria association is bound to improve muscle endurance, and in the end muscle endurance is what is needed to enhance mobility, independence, and quality of life in ageing.

Several question remain unanswered, and additional investigation in future years is required to better understand the molecular events that leads to the dynamic remodeling and re-positioning of the mitochondrial network with inactivity and activity, the dream being to develop strategies to improve CRU-mitochondria association and communications.

Supplementary Material

Refer to Web version on PubMed Central for supplementary material.

Acknowledgments

Funding

This work was supported by: a) Italian Telethon ONLUS Foundation (Rome, Italy): GGP13213 to FP; b) Italian Ministry of Health (Rome, Italy): GR: 2011–02352681 to SB; c) National Institute of Health (Bethesda, MD, U.S.A): AR059646–06 subcontract to FP.

Abbreviations:

ATP	adenoside triphosphate
CRU	Ca^{2+} release unit
EDL	extensor digitorum longus
EC coupling	excitation-contraction coupling
EM	electron microscopy
FDB	flexor digitorum brevis
IF	Immunofluorescence
RyR1	ryanodine receptor type 1

SERCA	sarco/endoplasmic reticulum ATPase
SR	sarcoplasmic reticulum
TT	transverse-tubule
WT	wild type

References

[1]. Paterson DH, Warburton DE, Physical activity and functional limitations in older adults: a systematic review related to Canada's Physical Activity Guidelines, Int. J. Behav. Nutr. Phys. Activ 7 (2010) 38.

[2]. Visser M, Schaap LA, Consequences of sarcopenia, Clin. Geriatr. Med 27 (3) (2011) 387–399. [PubMed: 21824554]

[3]. Roubenoff R, Hughes VA, Sarcopenia: current concepts, J. Gerontol. A Biol. Sci. Med. Sci 55 (12) (2000) M716–M724. [PubMed: 11129393]

[4]. Evans WJ, What is sarcopenia? J. Gerontol. A Biol. Sci. Med. Sci (1995) 50 Spec No:5–8. [PubMed: 7493218]

[5]. Schneider EL, Guralnik JM, The aging of America. Impact on health care costs, J. Am. Med. Assoc 263 (17) (1990) 2335–2340.

[6]. Franzini-Armstrong C, Jorgensen AO, Structure and development of E-C coupling units in skeletal muscle, Annu. Rev. Physiol 56 (1994) 509–534. [PubMed: 8010750]

[7]. Schneider H, Fallert M, Wachsmuth ED, Kinetics of intracellular Ca2+ concentration changes and cell contraction of electrically stimulated cardiomyocytes as analysed by automated digital-imaging microscopy, J. Microsc 175 (Pt 2) (1994) 108–120. [PubMed: 7966251]

[8]. Melzer W, Herrmann-Frank A, Luttgau HC, The role of Ca2+ ions in excitation-contraction coupling of skeletal muscle fibres, Biochim. Biophys. Acta 1241 (1) (1995) 59–116. [PubMed: 7742348]

[9]. Brookes PS, Yoon Y, Robotham JL, Anders MW, Sheu SS, Calcium, ATP, and ROS: a mitochondrial love-hate triangle, Am. J. Physiol. Cell Physiol 287 (4) (2004) C817–C833. [PubMed: 15355853]

[10]. Boncompagni S, Rossi AE, Micaroni M, Beznoussenko GV, Polishchuk RS, Dirksen RT, Protasi F, Mitochondria are linked to calcium stores in striated muscle by developmentally regulated tethering structures, Mol. Biol. Cell 20 (3) (2009) 1058–1067. [PubMed: 19037102]

[11]. Bolanos P, Guillen A, Rojas H, Boncompagni S, Caputo C, The use of Calcium orange-5N as a specific marker of mitochondrial Ca2+ in mouse skeletal muscle fibers, Pflügers Archiv 455 (4) (2008) 721–731. [PubMed: 17705046]

[12]. Rossi AE, Boncompagni S, Dirksen RT, Sarcoplasmic reticulum-mitochondrial symbiosis: bidirectional signaling in skeletal muscle, Exerc. Sport Sci. Rev 37 (1) (2009) 29–35. [PubMed: 19098522]

[13]. Rossi AE, Boncompagni S, Wei L, Protasi F, Dirksen RT, Differential impact of mitochondrial positioning on mitochondrial Ca(2+) uptake and Ca(2+) spark suppression in skeletal muscle, Am. J. Physiol. Cell Physiol 301 (5) (2011) C1128–C1139. [PubMed: 21849670]

[14]. Ashley Z, Sutherland H, Lanmuller H, Russold MF, Unger E, Bijak M, Mayr W, Boncompagni S, Protasi F, Salmons S, Jarvis JC, Atrophy, but not necrosis, in rabbit skeletal muscle denervated for periods up to one year, Am. J. Physiol. Cell Physiol 292 (1) (2007) C440–C451. [PubMed: 17218372]

[15]. Pietrangelo L, D'Incecco A, Ainbinder A, Michelucci A, Kern H, Dirksen RT, Boncompagni S, Protasi F, Age-dependent uncoupling of mitochondria from Ca2(+) release units in skeletal muscle, Oncotarget 6 (34) (2015) 35358–35371. [PubMed: 26485763]

[16]. Zampieri S, Pietrangelo L, Loefler S, Fruhmann H, Vogelauer M, Burggraf S, Pond A, Grim-Stieger M, Cvecka J, Sedliak M, Tirpakova V, Mayr W, Sarabon N, et al., Lifelong physical

exercise delays age-associated skeletal muscle decline, J. Gerontol. A Biol. Sci. Med. Sci 70 (2) (2015) 163–173. [PubMed: 24550352]

[17]. WHO, WHO The World Health Report (WHO)2007 - a Safer Future: Global Public Health Security in the 21st Century, (2008).

[18]. Haskell WL, Lee IM, Pate RR, Powell KE, Blair SN, Franklin BA, Macera CA, Heath GW, Thompson PD, Bauman A, Physical activity and public health: updated recommendation for adults from the American College of Sports Medicine and the American Heart Association, Med. Sci. Sports Exerc 39 (8) (2007) 1423–1434. [PubMed: 17762377]

[19]. Colberg SR, Sigal RJ, Prescribing exercise for individuals with type 2 diabetes: recommendations and precautions, Physician Sportsmed. 39 (2) (2011) 13–26.

[20]. Loud AV, A quantitative stereological description of the ultrastructure of normal rat liver parenchymal cells, J. Cell Biol 37 (1) (1968) 27–46. [PubMed: 5645844]

[21]. Mobley BA, Eisenberg BR, Sizes of components in frog skeletal muscle measured by methods of stereology, J. Gen. Physiol 66 (1) (1975) 31–45. [PubMed: 1159401]

[22]. Connolly AM, Keeling RM, Mehta S, Pestronk A, Sanes JR, Three mouse models of muscular dystrophy: the natural history of strength and fatigue in dystrophin-, dystrophin/utrophin-, and laminin alpha2-deficient mice, Neuromuscul. Disord 11 (8) (2001) 703–712. [PubMed: 11595512]

[23]. Boncompagni S, Michelucci A, Pietrangelo L, Dirksen RT, Protasi F, Exercise-dependent formation of new junctions that promote STIM1-Orai1 assembly in skeletal muscle, Sci. Rep 7 (1) (2017) 14286. [PubMed: 29079778]

[24]. Michelucci A, Paolini C, Canato M, Wei-Lapierre L, Pietrangelo L, De Marco A, Reggiani C, Dirksen RT, Protasi F, Antioxidants Protect Calsequestrin-1 Knockout Mice from Halothane- and Heat-induced Sudden Death, Anesthesiology, 2015.

[25]. Michelucci A, De Marco A, Guarnier FA, Protasi F, Boncompagni S, Antioxidant treatment reduces formation of structural cores and improves muscle function in RYR1(Y522S/WT) mice, Oxid. Med. Cell. Longev 2017 (2017) 6792694. [PubMed: 29062463]

[26]. Mammucari C, Gherardi G, Zamparo I, Raffaello A, Boncompagni S, Chemello F, Cagnin S, Braga A, Zanin S, Pallafacchina G, Zentilin L, Sandri M, De Stefani D, et al., The mitochondrial calcium uniporter controls skeletal muscle trophism in vivo, Cell Rep. 10 (8) (2015) 1269–1279. [PubMed: 25732818]

[27]. Schindelin J, Arganda-Carreras I, Frise E, Kaynig V, Longair M, Pietzsch T, Preibisch S, Rueden C, Saalfeld S, Schmid B, Tinevez JY, White DJ, Hartenstein V, et al., Fiji: an open-source platform for biological-image analysis, Nat. Methods 9 (7) (2012) 676–682. [PubMed: 22743772]

[28]. Schiaffino S, Reggiani C, Fiber types in mammalian skeletal muscles, Physiol. Rev 91 (4) (2011) 1447–1531. [PubMed: 22013216]

[29]. Ogino K, Wang DH, Biomarkers of oxidative/nitrosative stress: an approach to disease prevention, Acta Med. Okayama 61 (4) (2007) 181–189. [PubMed: 17726507]

[30]. Grune T, Merker K, Jung T, Sitte N, Davies KJ, Protein oxidation and degradation during postmitotic senescence, Free Radic. Biol. Med 39 (9) (2005) 1208–1215. [PubMed: 16214036]

[31]. Powers SK, Duarte J, Kavazis AN, Talbert EE, Reactive oxygen species are signalling molecules for skeletal muscle adaptation, Exp. Physiol 95 (1) (2010) 1–9. [PubMed: 19880534]

[32]. Jung T, Engels M, Klotz LO, Kroncke KD, Grune T, Nitrotyrosine and protein carbonyls are equally distributed in HT22 cells after nitrosative stress, Free Radic. Biol. Med 42 (6) (2007) 773–786. [PubMed: 17320760]

[33]. Marklund S, Marklund G, Involvement of the superoxide anion radical in the autoxidation of pyrogallol and a convenient assay for superoxide dismutase, Eur. J. Biochem 47 (3) (1974) 469–474. [PubMed: 4215654]

[34]. McCord JM, Fridovich I, Superoxide dismutase. An enzymic function for erythrocuprein (hemocuprein), J. Biol. Chem 244 (22) (1969) 6049–6055. [PubMed: 5389100]

[35]. Fridovich I, Superoxide anion radical (O2-.), superoxide dismutases, and related matters, J. Biol. Chem 272 (30) (1997) 18515–18517. [PubMed: 9228011]

[36]. Higuchi M, Cartier LJ, Chen M, Holloszy JO, Superoxide dismutase and catalase in skeletal muscle: adaptive response to exercise, J. Gerontol 40 (3) (1985) 281–286. [PubMed: 3989240]

[37]. Mastaloudis A, Leonard SW, Traber MG, Oxidative stress in athletes during extreme endurance exercise, Free Radic. Biol. Med 31 (7) (2001) 911–922. [PubMed: 11585710]

[38]. Knez WL, Jenkins DG, Coombes JS, The effect of an increased training volume on oxidative stress, Int. J. Sports Med 35 (1) (2014) 8–13. [PubMed: 23839729]

[39]. Chandwaney R, Leichtweis S, Leeuwenburgh C, Ji LL, Oxidative stress and mitochondrial function in skeletal muscle: effects of aging and exercise training, Age (Omaha). 21 (3) (1998) 109–117. [PubMed: 23604368]

[40]. Leick L, Lyngby SS, Wojtaszewski JF, Pilegaard H, PGC-1 alpha is required for training-induced prevention of age-associated decline in mitochondrial enzymes in mouse skeletal muscle, Exp. Gerontol 45 (5) (2010) 336–342. [PubMed: 20085804]

[41]. Rudolf R, Mongillo M, Magalhaes PJ, Pozzan T, In vivo monitoring of Ca(2+) uptake into mitochondria of mouse skeletal muscle during contraction, J. Cell Biol 166 (4) (2004) 527–536. [PubMed: 15314066]

[42]. Rizzuto R, Brini M, Murgia M, Pozzan T, Microdomains with high Ca2+ close to IP3-sensitive channels that are sensed by neighboring mitochondria, Science 262 (5134) (1993) 744–747. [PubMed: 8235595]

[43]. Pellegrino C, Franzini C, An electron microscope study of denervation atrophy in red and white skeletal muscle fibers, J. Cell Biol 17 (2) (1963) 327–349. [PubMed: 19866627]

[44]. Lu DX, Huang SK, Carlson BM, Electron microscopic study of long-term denervated rat skeletal muscle, Anat. Rec 248 (3) (1997) 355–365. [PubMed: 9214553]

[45]. Salmons S, Gale DR, Sreter FA, Ultrastructural aspects of the transformation of muscle fibre type by long term stimulation: changes in Z discs and mitochondria, J. Anat 127 (Pt 1) (1978) 17–31. [PubMed: 151671]

[46]. Hoppins S, Lackner L, Nunnari J, The machines that divide and fuse mitochondria, Annu. Rev. Biochem 76 (2007) 751–780. [PubMed: 17362197]

[47]. de Brito OM, Scorrano L, Mitofusin 2 tethers endoplasmic reticulum to mitochondria, Nature 456 (7222) (2008) 605–610. [PubMed: 19052620]

[48]. Merkwirth C, Langer T, Mitofusin 2 builds a bridge between ER and mitochondria, Cell 135 (7) (2008) 1165–1167. [PubMed: 19109886]

[49]. Santel A, Fuller MT, Control of mitochondrial morphology by a human mitofusin, J. Cell Sci 114 (Pt 5) (2001) 867–874. [PubMed: 11181170]

[50]. Ainbinder A, Boncompagni S, Protasi F, Dirksen RT, Role of Mitofusin-2 in mitochondrial localization and calcium uptake in skeletal muscle, Cell Calcium 57 (1) (2015) 14–24. [PubMed: 25477138]

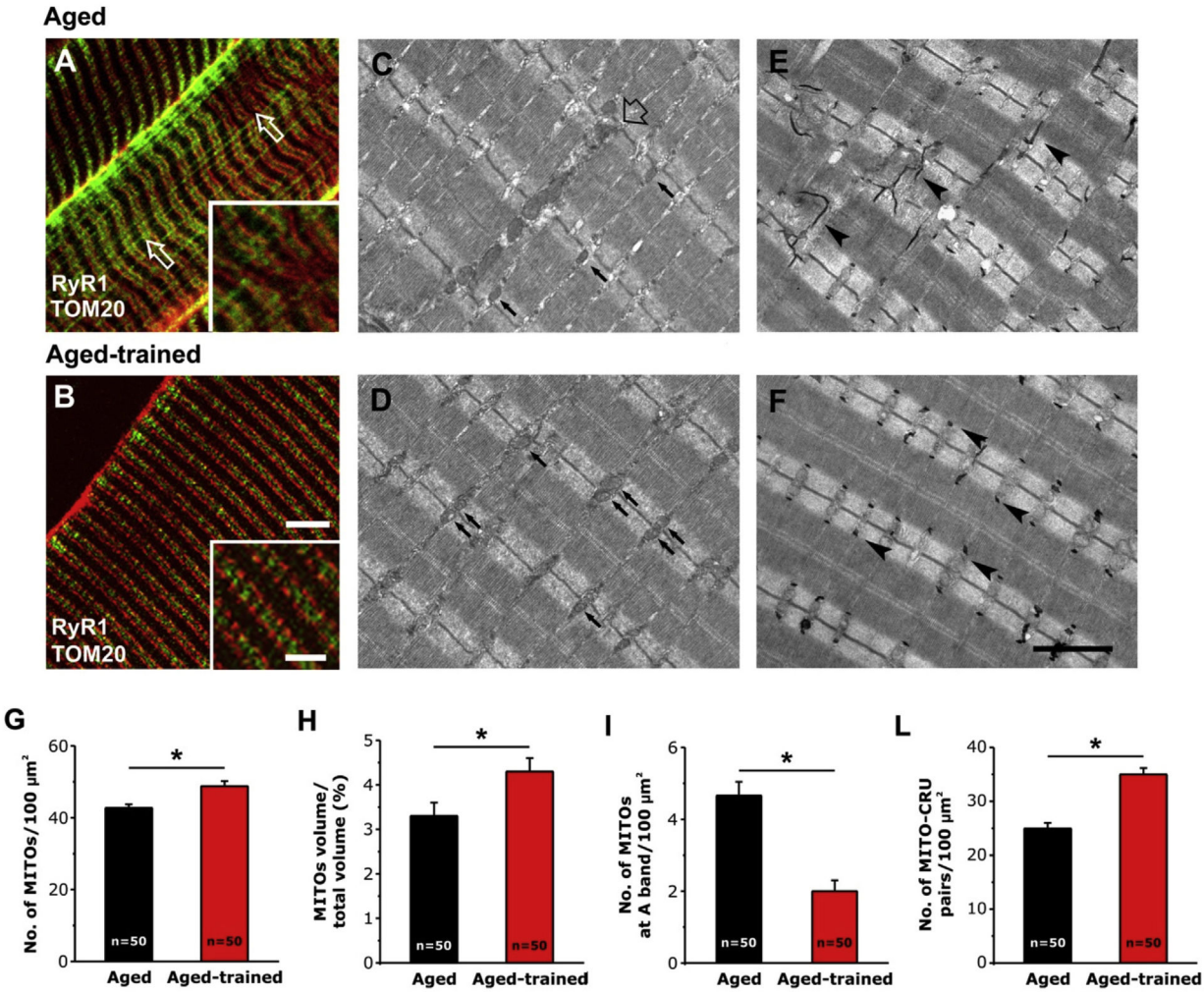

Fig. 1.

IF and EM analysis of EDL fibers from aged and aged-trained mice. A and B) Representative IF images showing RyR1 and TOM20 double-staining (marking the position of CRUs and mitochondria, respectively). C-F) Representative EM images showing the position of mitochondria (pointed by small arrows in C and D) and the organization of TTs (pointed by arrowheads in E and F). In C, the empty arrow point to an area with abnormal mitochondria distribution. G-L) Quantitative analysis of mitochondrial n./area, volume, disposition, and association with CRUs. Data are shown as mean ± SEM; n = number of EDL fibers analyzed; *$p < 0.05$ as evaluated by two-tailed unpaired Student's t-test. Scale bars: A and B, 5 µm (insets 2 µm); C–F, 2 µm.

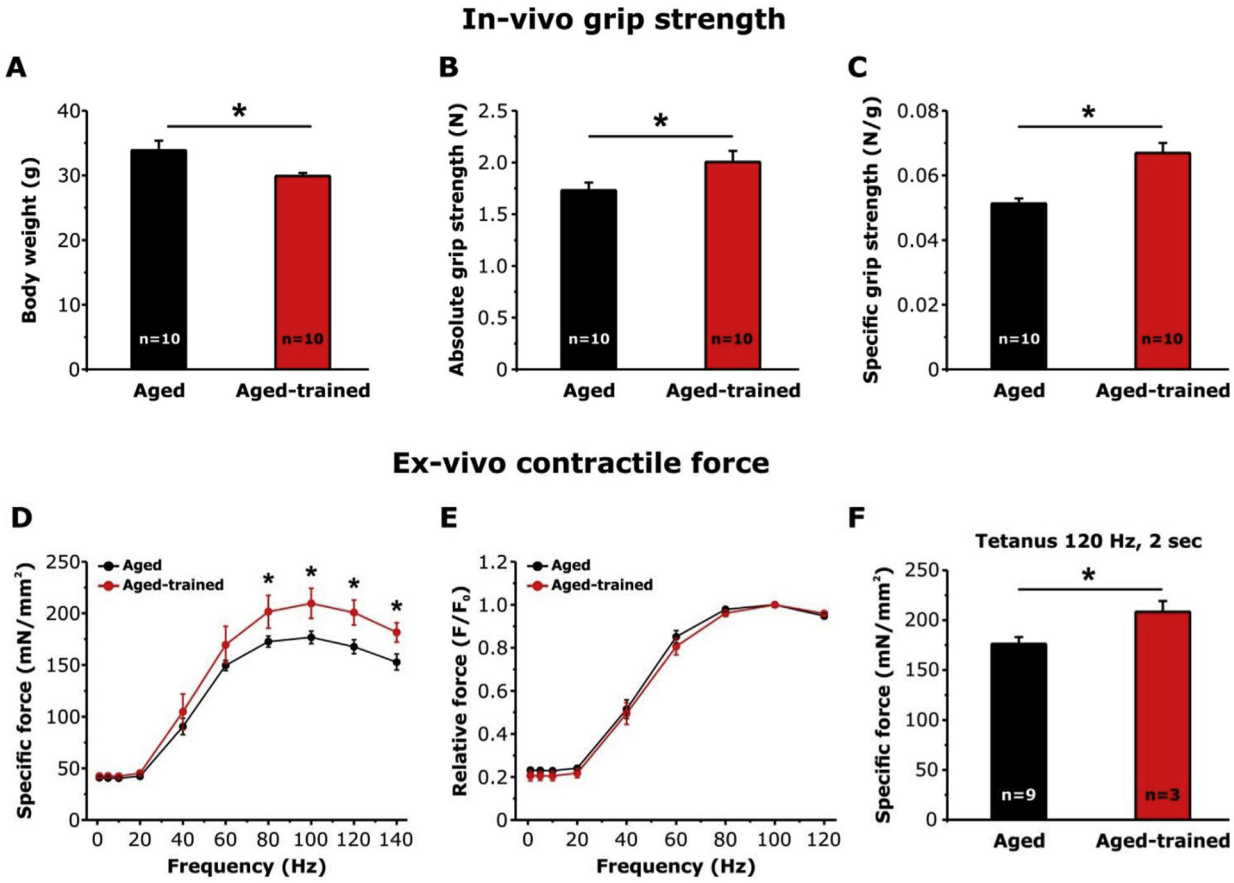

Fig. 2.

Measurements of in-vivo grip-strength and ex-vivo contractile force of EDL muscles in aged and aged-trained mice. A-C) Average body weight, and absolute and specific grip strength. D-E) Specific and relative (normalized to the maximal force at 100 Hz) force-frequency curves obtained from isolated EDL muscles by applying stimulus trains from 1 to 140 Hz. F) Specific force during a single 2 s, 120 Hz tetanic stimulation recorded for the same EDL muscles showed in (D). Data are shown as mean ± SEM; n = number of mice (A–C); n = number of EDL muscles analyzed (D–F); *$p < 0.01$ as evaluated by two-tailed unpaired Student's t-test in A-C and F. *$p < 0.05$ as evaluated by repeated measurements ANOVA followed by post-hoc Tukey test in D and E.

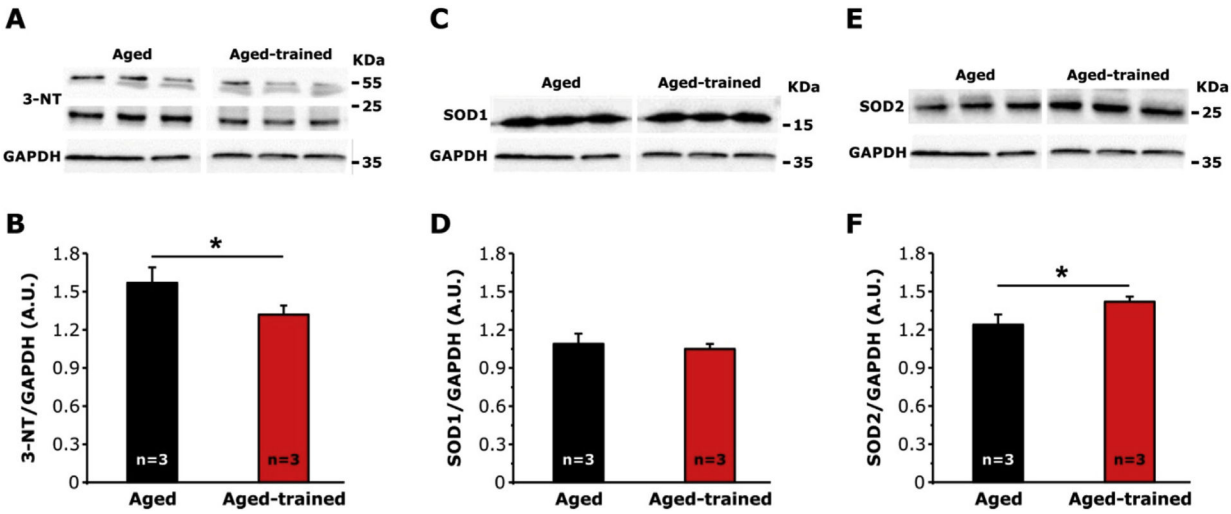

Fig. 3.

Levels of 3-Nitrotyrosine (3-NT), copper/zinc (SOD1), and manganese (SOD2) superoxide dismutase in muscle homogenates from aged and aged-trained mice. A, C and E) Representative immunoblots showing levels of 3-NT (A), SOD1 (C), and SOD2 (E) in hind limb muscle homogenates. B, D and F) Relative band densities of 3-NT (B), SOD1 (D), and SOD2 (F) normalized to GAPDH. Data are shown as mean ± SEM; n = number of mice; *p < 0.05 as evaluated by two-tailed unpaired Student's t-test.

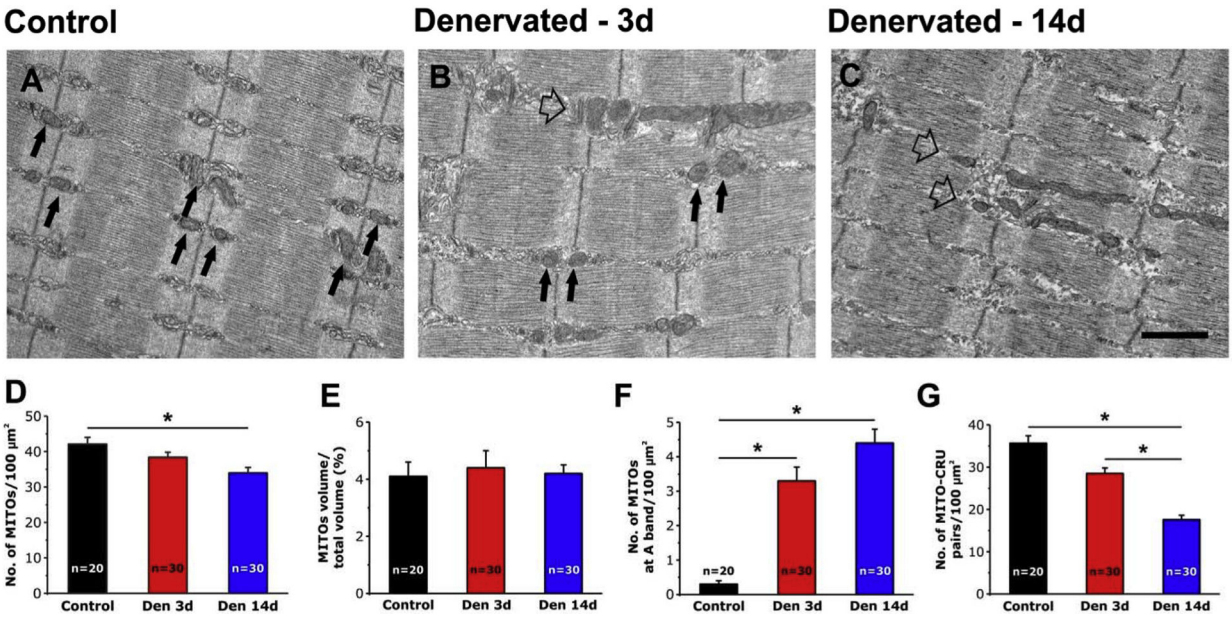

Fig. 4.

EM analysis of EDL fibers from control and denervated mice. A-C) Representative EM images showing EDL fibers from control mice (A), and from mice after 3 (B) and 14 (C) days of denervation. Black arrows point to mitochondria placed in the correct I band position, while empty arrows point to mitochondria forming longitudinal columns between myofibrils. D-G) Quantitative analysis of mitochondrial n./area, volume, disposition, and association with CRUs. Data are shown as mean ± SEM; n = number of EDL fibers analyzed; *$p < 0.01$ as evaluated by one-way ANOVA followed by post-hoc Tuckey test. Scale bars: A-C, 1 µm.

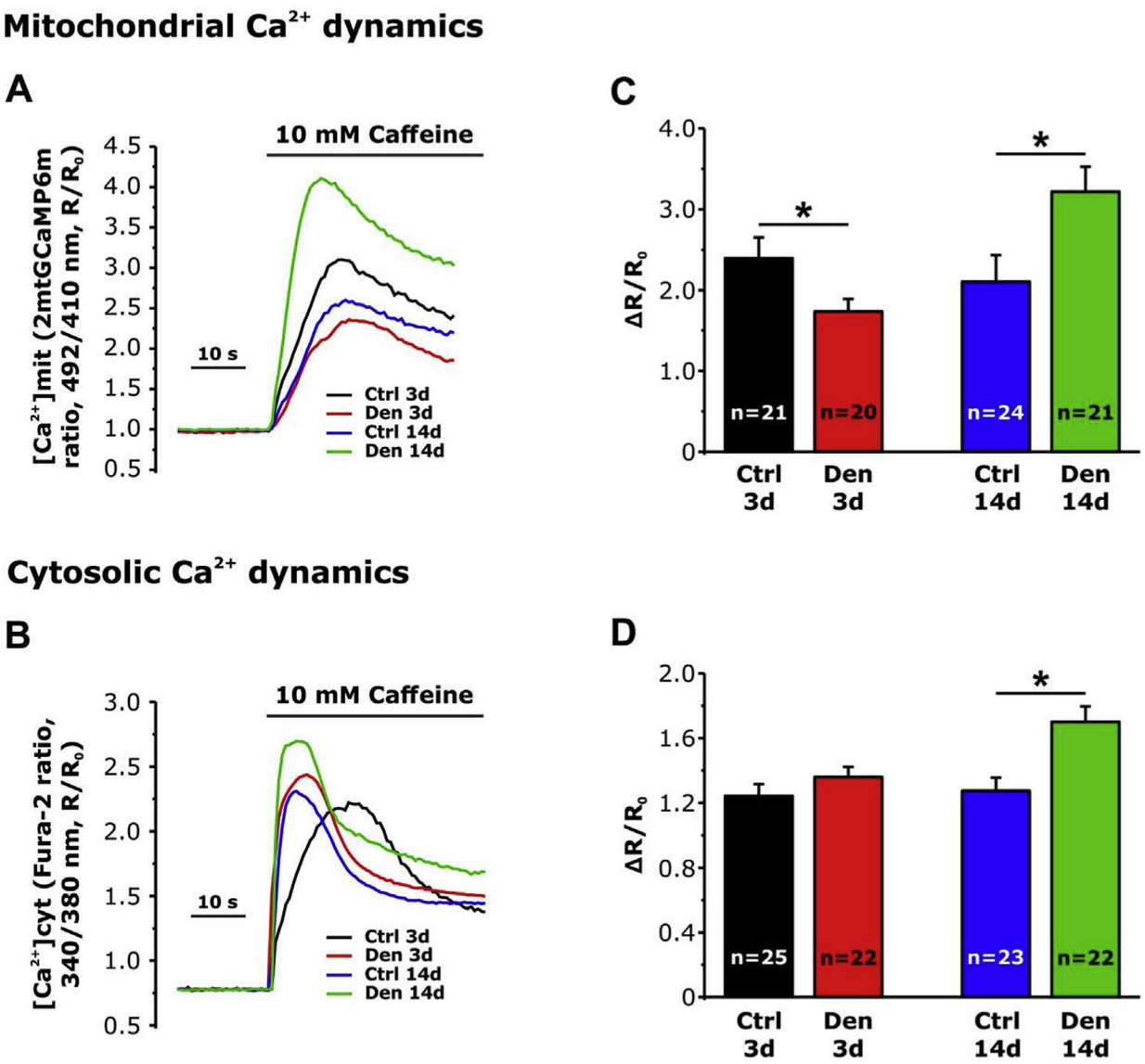

Fig. 5.

Mitochondrial and cytosolic Ca^{2+} dynamics in single FDB fibers from control and denervated mice. A and B) Representative traces of mitochondrial and cytosolic Ca^{2+} dynamics following application of 10 mM of caffeine, recorded in FDB fibers from control mice and from mice at 3 and 14 days of denervation. C and D) Average mitochondrial and cytosolic Ca^{2+} levels. Data are shown as mean ± SEM; *$p < 0.05$ as evaluated by two-tailed unpaired Student's t-test.

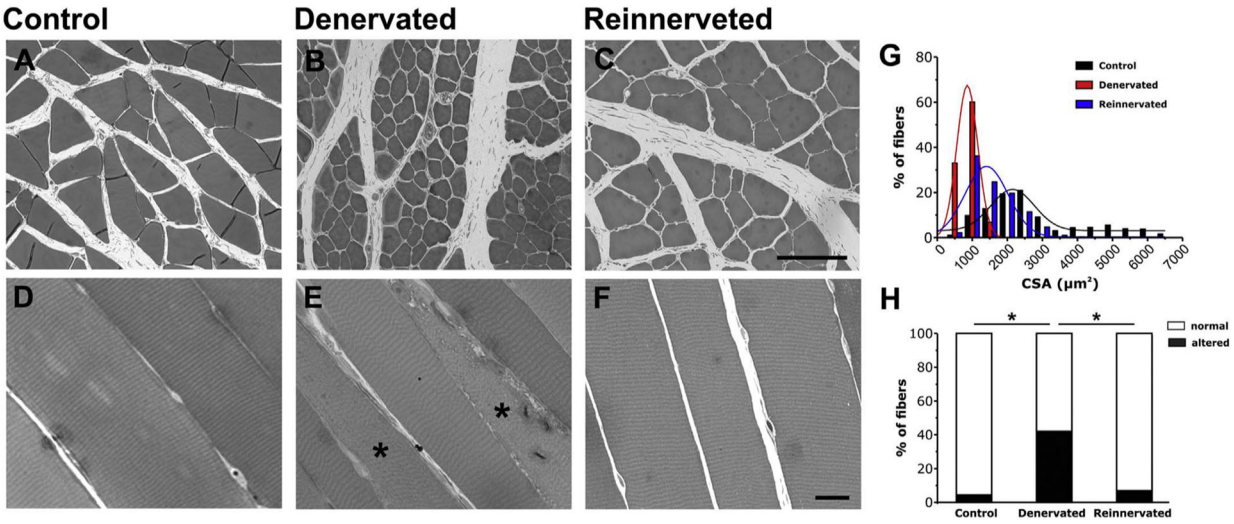

Fig. 6.

Histological analysis of EDL fibers from control, denervated and reinnervated rats. A-F) Representative histological images of transversal (A–C) and longitudinal (D–F) sections of EDL muscle fibers from control (A and B), denervated (C and D) and reinnervated (E and F) rats. Asterisk in E indicates fibers with internal areas with disarray of striation. G) Distribution frequency of CSA of EDL fibers. H) Percentage of fibers classified as normal (white) or altered (black). n = number of EDL fibers analyzed; *$p < 0.01$ as evaluated by one-way ANOVA followed by post-hoc Tuckey test. Scale bars: A-C, 100 µm; D-F, 20 µm.

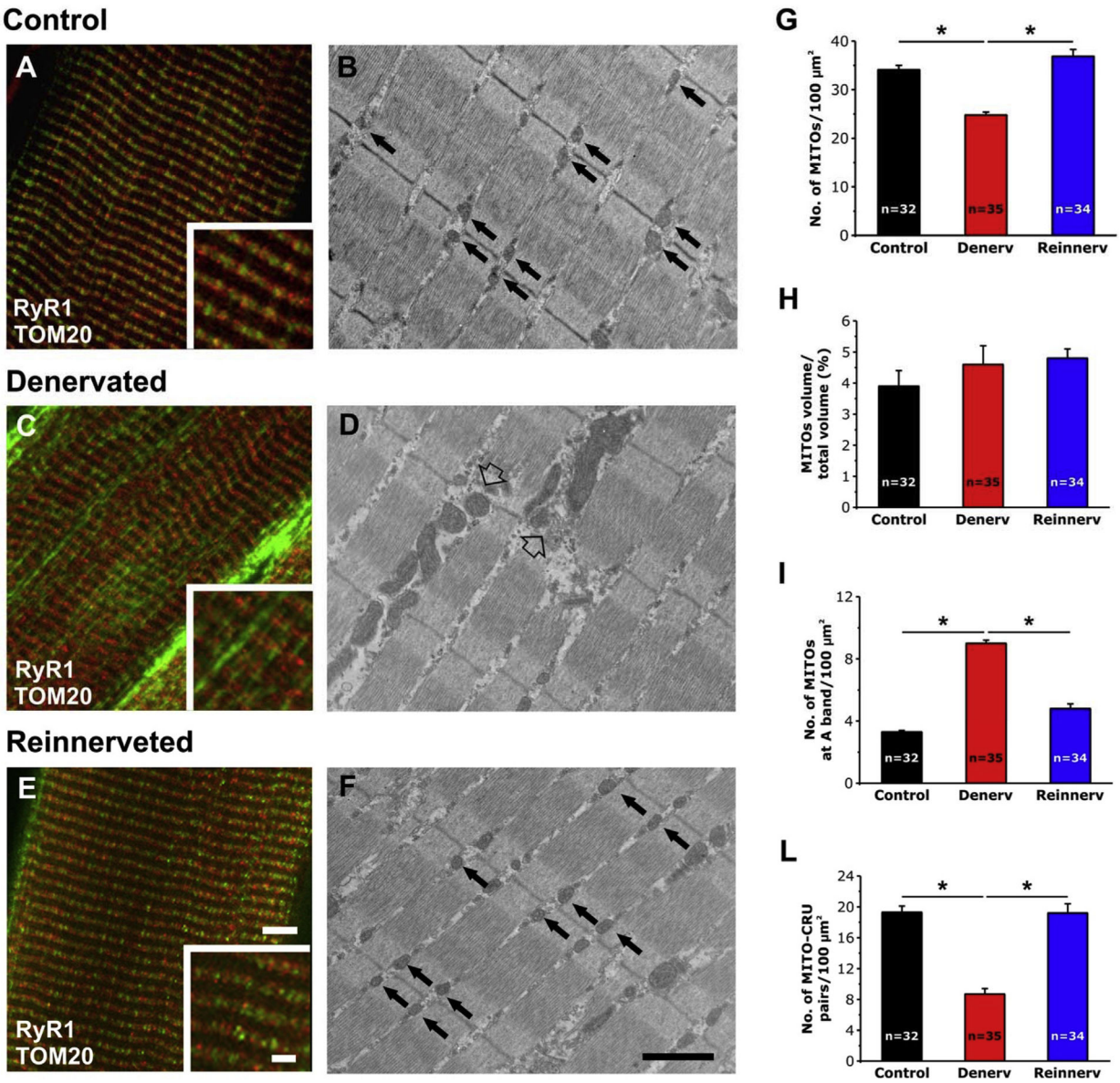

Fig. 7.

IF and EM analysis of EDL fibers from control, denervated, and reinnervated rats. A, C and E) Representative IF images showing fibers double immuno-labeled with RyR1 and TOM20 antibodies marking the position of CRUs and mitochondria, respectively. B, D and F) Representative EM images showing the disposition of mitochondria in EDL fibers from control, denervated, and reinnervated rats. In B and F black arrows point to mitochondria properly positioned at the I band, while in D empty arrows point to mitochondria forming longitudinal columns between myofibrils. G-L) Quantitative analysis of mitochondrial n./ area, volume, disposition, and association with CRUs. Data are shown as mean ± SEM; n = number of fibers analyzed; *$p < 0.05$ as evaluated by one-way ANOVA followed by post-hoc Tuckey test. Scale bars: A, C and E, 5 µm (insets 2 µm); B, D and F, 1 µm.

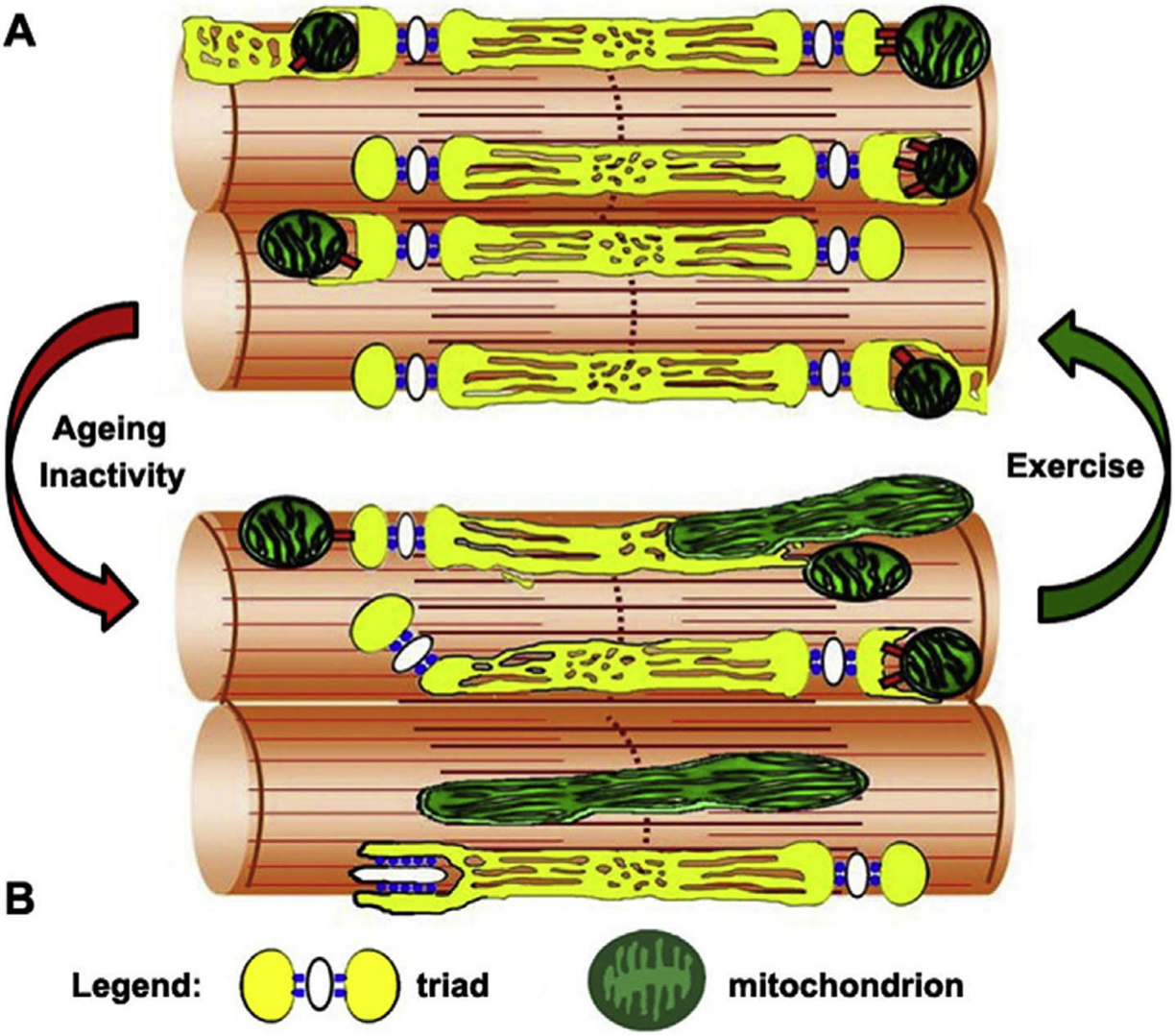

Fig. 8.

Graphical model summarizing the alterations caused by age and/or inactivity (red arrow) to CRUs and mitochondria morphology and distribution, changes that are reverted/prevented by exercise (green arrow). A) Modelling of normal morphology and distribution of mitochondria and CRUs in adult or exercised muscle. B) Modelling of altered distribution and morphology of mitochondria and CRUs caused by ageing and/inactivity. (For interpretation of the references to colour in this figure legend, the reader is referred to the Web version of this article.)

Table 1

Quantitative EM analyses of n./area, orientation, and morphology of CRUs in EDL muscles from mice. Note: data in parenthesis are from Pietrangelo et al., 2015.

	A	B	C	D
	No. of CRUs/100 μm^2	**% of Oblique CRUs**	**% of Longitudinal CRUs**	**% of Dyads**
Aged	(74.1 ± 1.1)	(8.7 ± 0.8)	(0.9 ± 0.2)	(4.0 ± 0.4)
Aged-trained	85.5 ± 2.0*	5.1 ± 0.7*	0.7 ± 0.3	0.6 ± 0.4*

Data are shown as mean ± SEM (*$p < 0.01$).

Samples size: 50 fibers from 5 aged mice, 50 fibers from 5 aged-trained mice; Columns A, C and D: 10 micrographs/fiber; Column B: 2 micrographs/fiber (low magnification images in transversal sections).

Table 2

Quantitative EM analyses of n./area, orientation, and morphology of CRUs in EDL muscles from denervated mice.

	A	B	C	D
	No. of CRUs/100 μm^2	**% of Oblique CRUs**	**% of Longitudinal CRUs**	**% of Dyads**
Control	93.3 ± 2.4	6.6 ± 3.7	0.6 ± 0.1	0.6 ± 0.1
Denervated - 3 days	79.2 ± 1.6*	9.8 ± 0.9*	0.5 ± 0.2	1.4 ± 0.3*
Denervated - 14 days	62.0 ± 2.3*&	17.6 ± 3.3*&	3.3 ± 1.1*&	2.5 ± 0.7*&

Data are shown as mean ± SEM (*$p < 0.01$ vs. control; & $p < 0.01$ vs. denervated for 3 days).

Samples size: 20 fibers from 2 Control CD1 mice, 20 fibers from 2 mice denervated for 3 days, 20 fibers from 2 mice denervated for 14 days; Columns AD: 5 micrographs/fiber.